Electronic Supplementary Information

In situ confined-synthesis of mesoporous FeS_2@C superparticles and their enhanced sodium-ion storage properties

Luyin Yao,[a,b] Biwei Wang,[b] Yuchi Yang,[a] Xiao Chen,[a] Jianhua Hu,[a] Dong Yang*[a] and Angang Dong*[b]

a. State Key Laboratory of Molecular Engineering of Polymers and Department of Macromolecular Science, Fudan University, Shanghai 200433, China.

b. iChem, Shanghai Key Laboratory of Molecular Catalysis and Innovative Materials, and Department of Chemistry, Fudan University, Shanghai 200433, China.

Experimental Section

The Synthesis and Self-Assembly of Fe_3O_4 NPs. In brief, Fe_3O_4 NPs were synthesized according to the procedure reported previously.[1] To assemble the superparticles, Fe_3O_4 NPs in hexane were added into an aqueous solution of dodecyltrimethylammonium bromide (DTAB). Then, the mixture was subjected to homogenization to form an oil-in-water system. After that, the mixture was heated at 50 °C under mechanical stirring to remove hexane. The as-synthesized Fe_3O_4 NPs superlattices were collected by a magnet and washed by deionized water.

The Preparation of FeS_2@C SPs. The Fe_3O_4 NPs superlattices were heated at 500 °C in Ar for 2 h to carbonize OA ligands. The carbonized Fe_3O_4 SPs were treated by 1 M HCl solution for 2 h to partially etch Fe_3O_4 NPs (denoted as Fe_3O_4@C-2 SPs). The resulting Fe_3O_4@C-2 SPs were washed several times with water followed by drying under vacuum for 6 h.

FeS_2@C-2 SPs were fabricated by the reaction between Fe_3O_4@C-2 SPs and

sulfur powder. In a typical procedure, the mixture of Fe_3O_4@C-2 SPs and sulfur powder was heated at 400 °C under Ar for 3 h. After cooling to room temperature, the resulting FeS_2@C-2 SPs were rinsed with carbon disulfide and then washed with water and ethanol several times. The purified FeS_2@C-2 SPs were then dried at 90 °C under vacuum for 12 h. FeS_2@C-0 SPs were synthesized through a similar procedure without the partial etching of Fe_3O_4 NPs.

Material Characterization Powder X-ray diffraction (XRD, X'pert PRO, Cu Kα radiation), field-emission scanning electron microscopy (SEM, Zeiss Ultra-55, 5 kV), and transmission electron microscopy (TEM, Tecnai G2 20 TWIN, 200 kV) were used to characterize the structure and morphology of the as-prepared samples. Thermogravimetric analysis (TGA, TGA1 Mettler Toledo) was carried out to determine the content of the active material. The porosity and Brunauer-Emment-Teller (BET) surface area were determined by N_2 adsorption/desorption measurements (TristarII3020). Leica EM TIC 3X argon ion cutter was used to cut the cross-sections of the electrodes.

Electrochemical Measurements The electrochemical performances of the materials were evaluated by using the 2016-type coin cells which were assembled in an Ar-filled glove box. Sodium foils were used as the counter electrodes， and glass fibres (Whatman, CAT NO. 1825-090) were used as the separator. 1 M $NaSO_3CF_3$ in diglyme (DGM) was used as the electrolyte. The slurry for making the working electrodes was prepared by mixing the active material, acetylene black, and polyvinylidene fluoride (PVDF) in a weight ratio of 70: 20: 10. The specific capacity was calculated based on the mass of active material. The slurry was coated onto Cu foil with a loading mass of ~ 1 mg cm^{-2} and was then dried at 90 °C under vacuum for 12 h. Galvanostatic tests were carried out on a Neware cell test system with a voltage range of 0.8-3 V. Cyclic voltammetry (CV) was performed on AUTOLAB potentiostat/galvanostat apparatus (N204) with a constant scan rate of 0.1 mV s^{-1}. Electrochemical impedance measurements (EIS) was tested at a 5 mV ac oscillation amplitude over the frequency range of 100 kHz to 100 MHz.

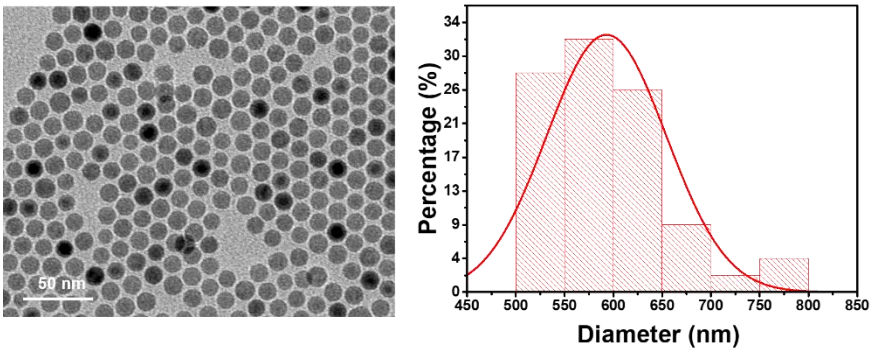

Fig. S1 (a) TEM image of Fe_3O_4 NPs used for making superparticles; (b) Size distribution histogram of Fe_3O_4@C SPs.

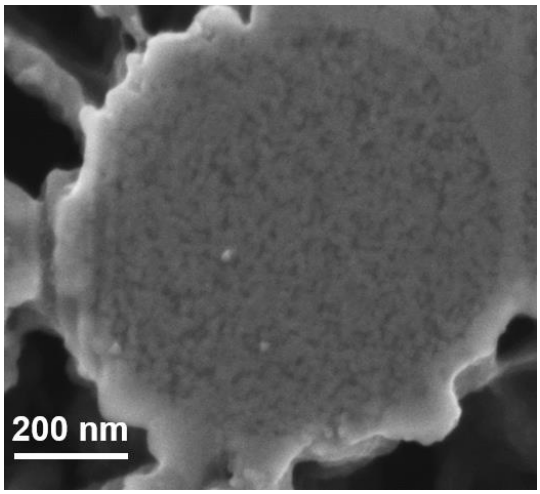

Fig. S2 Cross-sectional SEM image of a single FeS_2@C-0 SP, showing the more compact superstructure due to the growth of large FeS_2 NPs.

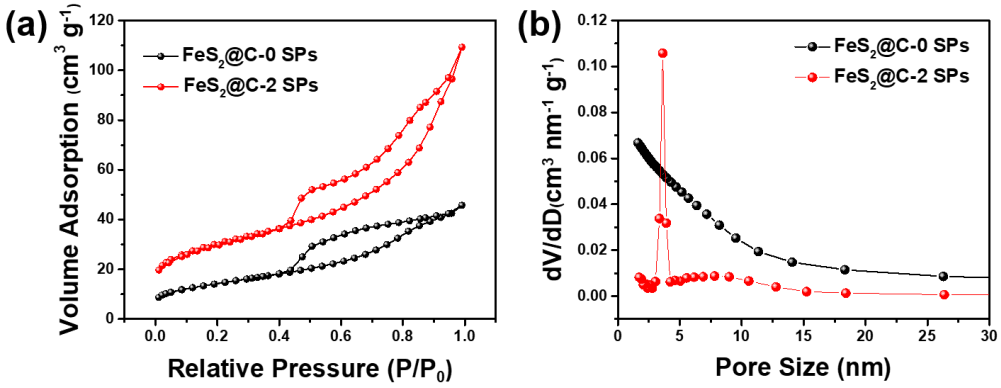

Fig. S3 (a) N_2 adsorption and desorption isotherms of FeS_2@C-2 SPs and FeS_2@C-0 SPs; (b) Pore size distribution of FeS_2@C-2 SPs and FeS_2@C-0 SPs, which was calculated from the desorption branch using the Barrett-Joyner-Halenda (BJH) model.

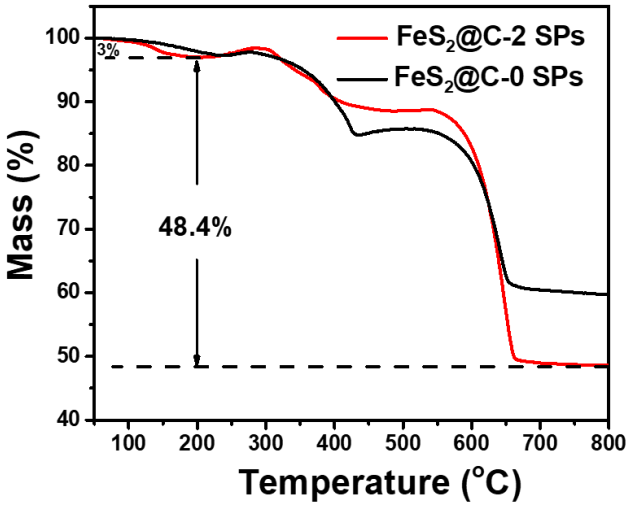

Fig. S4 TGA analysis of FeS_2@C-0 SPs and FeS_2@C-2 SPs at a temperature ramp of 10 ^oC min^{-1} in air.

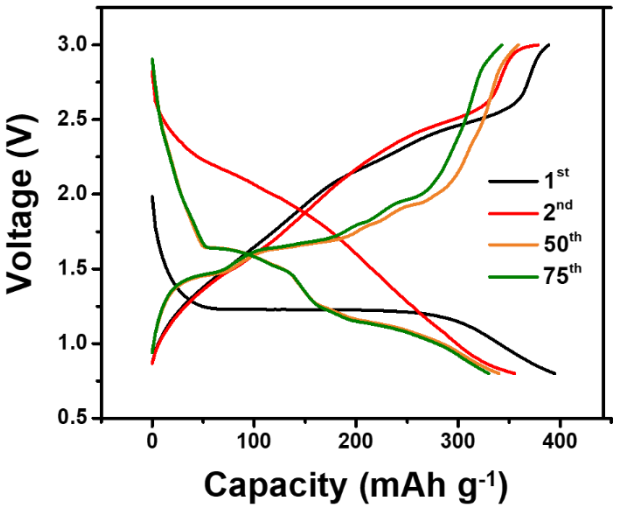

Fig. S5 Charge and discharge voltage profiles of FeS_2@C-2 SPs at a current density of 0.1 A g^{-1}.

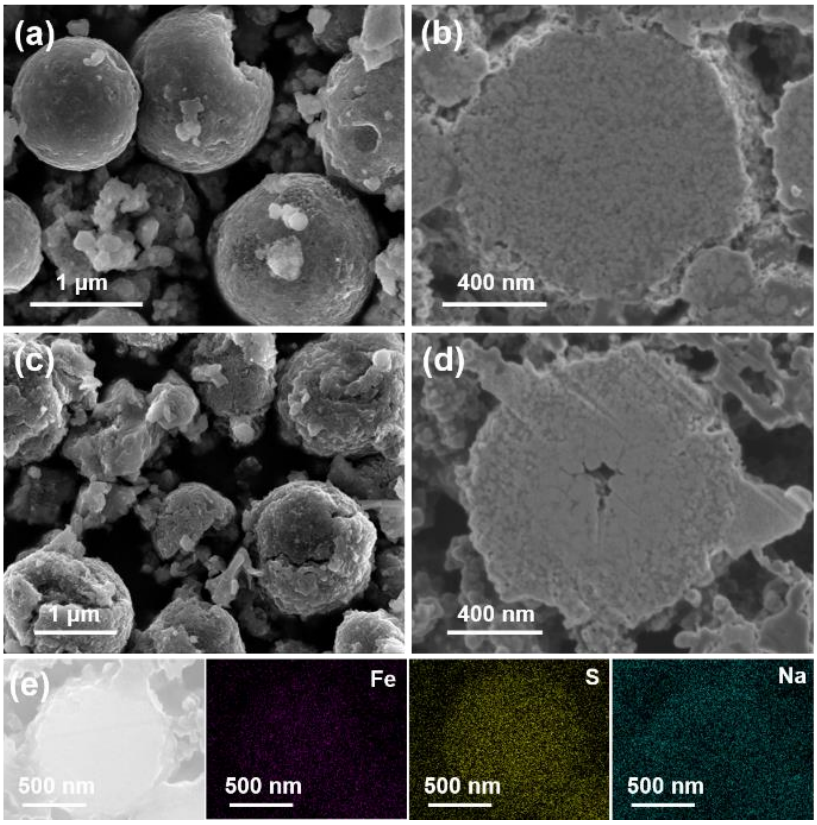

Fig. S6 SEM and cross-sectional SEM images of FeS_2@C-2 SPs (a, b) and FeS_2@C-0 SPs (c, d) after cycling. (e) Elemental mapping of FeS_2@C-2 SPs after cycling.

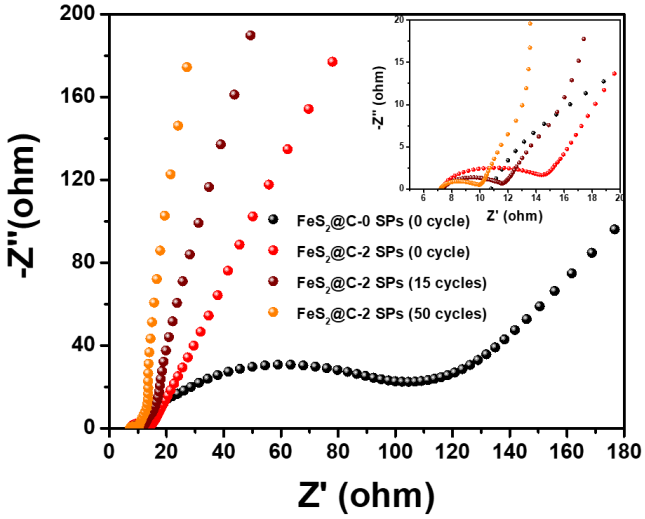

Fig. S7 Nyquist plots of FeS_2@C-0 SPs and FeS_2@C-2 SPs. Inset shows the magnified plots in the middle-frequency region.

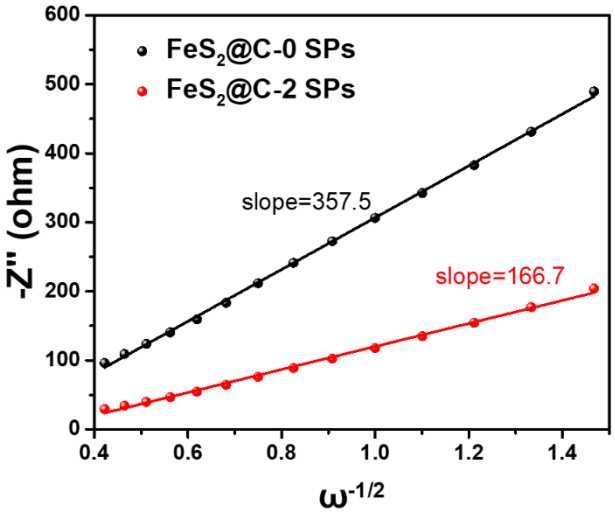

Fig. S8 The variations and fittings of –Z'' and $\omega^{-1/2}$ in the low-frequency region of FeS_2@C-0 SPs and FeS_2@C-2 SPs.

Diffusion Coefficient Calculation The value of apparent Na diffusion coefficient ($D_{apparent}$) can be calculated using the following equation eq 1, according to EIS data.[2]

$$D_{apparent}=R^2T^2/2A^2n^4F^4C^2\sigma^2 \quad (1)$$

$$-Z''=RD+RL+\sigma\omega^{-1/2} \quad (2)$$

In which R, T, A, n, F, C, and σ represent the gas constant (8.314 J K^{-1} mol^{-1}), absolute temperature (298 K), surface area of the electrode (1.3 cm^2), number of electrons per molecule during the redox process (n=1), Faraday's constant (96500 C mol^{-1}), the concentration of sodium ions (calculated from the density and the molecular weight of $NaFeS_2$, which is 1.59×10^{-2} mol cm^{-3}) and Warburg factor, respectively. The values of σ can be estimated in Fig. S8, where the ω is the angular frequency. The Na-ion diffusion coefficient of FeS_2@C-0 SPs and FeS_2@C-2 SPs are 6.48×10^{-16} and 2.98×10^{-15} cm^2 s^{-1}, respectively. This result confirms that FeS_2@C-2 SPs has a higher Na-ion diffusion coefficient due to the smaller NP size and rich void space within the superparticles.

Table S1 Electrochemical performance comparison between FeS_2@C-2 SPs and representative transition-metal-sulfide-based anode materials reported previously.

Types of materials	Voltage range (V)	Cycling performance	Rate capability	Ref.
FeS_2@C-2 SPs	0.8-3	83.4% of capacity retention after 1000 cycles at 0.2 A g^{-1} (329 mAh g^{-1})	244 mAh g^{-1} at 10 A g^{-1}, and 67.0% of capacity retention at 10 A g^{-1} compared with the capacity at 0.1 A g^{-1}	This work
		76.7% of capacity retention after 1000 cycles at 1 A g^{-1} (283 mAh g^{-1})		
		52.3% of capacity retention after 4000 cycles at 5 A g^{-1} (201 mAh g^{-1})		
FeS_2/rGO-A	0.8-3	58.03 % of capacity retention after 800 cycles at 0.9 A g^{-1}.	52.7% of capacity retention at 5C compared with the capacity at 0.1C.	3
Pyrite FeS_2	0.8-3	180 mAh g^{-1} after 20000 cycles at 1 A g^{-1}	170 mAh g^{-1} at 20 A g^{-1}	4
Cobalt-doped FeS_2	0.8-2.9	220 mAh g^{-1} after 5000 cycles at 2 A g^{-1}	192 mAh g^{-1} at 10 A g^{-1}	5
FeS_2@rGO	0.8-3	79.1% of capacity retention after 250 cycles at 0.5C. (240 mAh g^{-1})	192.9 mAh g^{-1} at 2C	6
FeS_2	0.6-3	415 mAh g^{-1} after 100 cycles at 0.06 A g^{-1}	290 mAh g^{-1} at 0.2 A g^{-1}.	7
FeS_2-PAA	0.5-3	87.8% of capacity retention after 800 cycles at 0.2 A g^{-1}. (460 mAh g^{-1})	323 mAh g^{-1} at 5 A g^{-1}	8
FeS_2 NCs	0.02-2.5	50% of capacity retention after 600 cycles at 1 A g^{-1}. (410 mAh g^{-1})	530 mAh g^{-1} after 100 cycles at 5 A g^{-1}	9
FeS_2@C	0.01-3	330 mAh g^{-1} after 800 cycles at 2 A g^{-1}	401 mAh g^{-1} at 5 A g^{-1}	10
FeS/C	0.01-2.3	67.6% of capacity retention after 300 cycles at 0.1 A g^{-1}	72.7% of capacity retention at 5C compared with the capacity at 0.2C	11
CoS_2 micro/nanostructures	1.0-3.0	~240 mAh g^{-1} over 800 cycles at 0.1 A g^{-1}		12
CoS_2/rGO	0.8-2.4	192 mAh g^{-1} after 1000 cycles at 1 A g^{-1}	202.7 mA h g^{-1} at 2 A g^{-1}	13
Ni_3S_2/rGo	0.01-3	71.7 % of capacity retention after 140 cycles at 0.3 A g^{-1}. (443mAh g^{-1})	74.8% of capacity retention at 3 A g^{-1} compared with the capacity at 0.2 A g^{-1}	14
MoS_2@C-CMC	0.01-3	286 mAh g^{-1} after 100 cycles at 0.08 A g^{-1}.	205 mA h g^{-1} at 1 A g^{-1}	15

References

1 J. Park, K. An, Y. Hwang, J.-G. Park, H.-J. Noh, J.-Y. Kim, J.-H. Park, N.-M. Hwang and T. Hyeon, *Nat. Mater.*, 2004, **3**, 891.

2 X. Y. Wang, H. Hao, J. L. Liu, T. Huang and A. S. Yu, *Electrochim. Acta*, 2011, **56**, 4065-4069.

3 W. H. Chen, S. H. Qi, L. Q. Guan, C. T. Liu, S. Z. Cui, C. Y. Shen and L. W. Mi, *J. Mater. Chem. A*, 2017, **5**, 5332-5341.
4 Z. Hu, Z. Q. Zhu, F. Y. Cheng, K. Zhang, J. B. Wang, C. C. Chen and J. Chen, *Energy Environmental Sci.*, 2015, **8**, 1309-1316.
5 K. Zhang, M. Park, L. M. Zhou, G.-H. Lee, J. Shin, Z. Hu, S. L. Chou, J. Chen and Y.-M. Kang, *Angew. Chem. Int. Ed.*, 2016, **55**, 12822-12826.
6 W. H. Chen, S. H. Qi, M. M. Yu, X. M. Feng, S. Z. Cui, J. M. Zhang and L. W. Mi, *Electrochim. Acta*, 2017, **230**, 1-9.
7 Y. J. Zhu, L. M. Suo, T. Gao, X. L. Fan, F. D. Han and C. S. Wang, *Electrochem. Commun.*, 2015, **54**, 18-22.
8 K. Y. Chen, W. X. Zhang, L. H. Xue, W. L. Chen, X. H. Xiang, M. Wan and Y. H. Huang, *ACS Appl. Mater. Interfaces*, 2017, **9**, 1536-1541.
9 M. Walter, T. Zund and M. V. Kovalenko, *Nanoscale*, 2015, **7**, 9158-9163.
10 Z. M. Liu, T. C. Lu, T. Song, X. Y. Yu, X. W. Lou and U. Paik, *Energy Environmental Sci.*, 2017, **10**, 1576-1580.
11 Y. X. Wang, J. P. Yang, S. L. Chou, H. K. Liu, W. X. Zhang, D. Y. Zhao and S. X. Dou, *Nat. Commun.*, 2015, **6**, 8689.
12 X. Liu, K. Zhang, K. X. Lei, F. J. Li, Z. L. Tao and J. Chen, *Nano Res.*, 2016, **9**, 198-206.
13 Z. W. Li, W. J. Feng, Y. Q. Lin, X. Liu and H. L. Fei, *RSC Adv.*, 2016, **6**, 70632-70637.
14 G. D. Park, J. S. Cho and Y. C. Kang, *Nanoscale*, 2015, **7**, 16781-16788.
15 X. Q. Xie, T. Makaryan, M. Q. Zhao, K. L. Van Aken, Y. Gogotsi and G. X. Wang, *Adv. Energy Mater.*, 2016, **6**, 1502161.